Ab initio studies of spin-spiral waves and exchange interactions in 3*d* transition metal atomic chains

J. C. Tung[1] and G. Y. Guo[1,2,*]

[1]*Department of Physics and Center for Theoretical Sciences, National Taiwan University, Taipei 106, Taiwan, Republic of China*

[2]*Graduate Institute of Applied Physics, National Chengchi University, Taipei 116, Taiwan, Republic of China*

(Received 7 July 2010; revised manuscript received 8 January 2011; published 4 April 2011)

The total energy of the transverse spin-spiral wave as a function of the wave vector for all 3*d* transition metal atomic chains has been calculated within *ab initio* density functional theory with the generalized gradient approximation. It is predicted that at the equilibrium bond length, the V, Mn, and Fe chains have a stable spin-spiral structure, while the magnetic ground state of the Cr, Co, and Ni chains remains collinear. Furthermore, all the exchange interaction parameters of the 3*d* transition metal chains are evaluated by using the calculated energy dispersion relations of the spin-spiral waves. Interestingly, it is found that the magnetic couplings in the V, Mn, and Cr chains are frustrated (i.e., the second near-neighbor exchange interaction is antiferromagnetic), and this leads to the formation of the stable spin-spiral structure in these chains. The spin-wave stiffness constant of these 3*d* metal chains is also evaluated and is found to be smaller than its counterpart in bulk systems. The upper limit (on the order of 100 Kelvins) of the possible magnetic phase transition temperature in these atomic chains is also estimated within the mean-field approximation. The electronic band structure of the spin-spiral structures have also been calculated. It is hoped that the interesting findings here of the stable spin-spiral structure and frustrated magnetic interaction in the 3*d* transition metal chains will stimulate further theoretical and experimental research in this field.

DOI: 10.1103/PhysRevB.83.144403 PACS number(s): 71.70.Gm, 73.21.Hb, 75.10.−b, 75.30.Ds

I. INTRODUCTION

Noncollinear magnetism, especially spin-spiral structures, has received much attention in recent decades, not only for possible magnetism-based technological applications[1–3] but also for fundamental physics.[4–13] In particular, it was recently reported that spin chirality in geometrically frustrated pyrochlore compounds could generate magnetic monopoles[4,5] and also a large anomalous Hall effect.[10] It was also proposed recently that the spin-spiral structure could be the main source of the magnetoelectric effect observed recently in multiferroic oxides.[2,3] The spin-spiral structure, in which the magnetization rotates along a certain direction in a bulk material, was observed two decades ago in neutron-diffraction experiments on fcc Fe and $Fe_{100-x}Co_x$ alloy precipitates in Cu.[13] This experimental finding has since stimulated many *ab initio* studies of the spin-spiral structures in bulk magnets.[12,14–20] Indeed, *ab initio* calculations[12,17,19] corroborated that stable spin-spiral states exist in fcc Fe. Furthermore, *ab initio* total energy calculations for the spin-spiral structures also helped to formulate an explanation of the anomalous magnetovolume properties of the Invar alloys (the Invar effect).[14]

Noncollinear magnetism in low-dimensional systems has also been studied both theoretically and experimentally in recent years.[7,21–23] For example, the Mn monolayer on the W(001) surface was recently investigated[7] jointly by spin-polarized scanning tunneling microscopy and also *ab initio* calculations, and it was concluded that a spin-spiral structure along the (110) direction exists in this monolayer system. A stable spin-spiral structure with propagation vector $\mathbf{q} = (0,0,0.15)(2\pi/a)$ was also predicted to exist in the unsupported free-standing Fe(110) monolayer with the lattice constant of 3.16Å.[21,22] Co/CoPt bilayers were also found to support noncollinear spiral structures by Brillouin light scattering.[23] Interestingly, very recent *ab initio* calculations show that in Mn chains on Ni(001), the magnetic structure could change from noncollinear to collinear ferrimagnetic, depending on whether the number of Mn atoms is even or odd.[6]

Stimulated by possible unusual magnetism in one-dimensional (1D) systems, we have recently carried out systematic *ab initio* studies of the collinear magnetic properties of linear and zigzag atomic chains of all 3*d*,[24] 4*d*, and 5*d* (Ref. 25) transition metals. Although the ideal infinite free-standing 3*d* transition metal atomic chain is unstable and cannot be prepared experimentally, short suspended monostrand metal nanowires and atomic chains have been prepared in mechanical break junctions.[26–28] Furthermore, structurally stable Co atomic chains have recently been prepared on a vicinal Pt(997) surface[29] or inside nanotubes.[30] Therefore, we have also performed *ab initio* calculations for the 3*d* transition metal linear atomic chains on the Cu(001) surface[31,32] to understand how the substrates would affect the magnetic properties of the nanowires.

The purpose of the present work is to study possible spin-spiral structures in all 3*d* transition metal atomic chains by *ab initio* calculation of the total energy of the spin-spiral state as a function of propagation wave vector **q**. Indeed, we find that the magnetic ground state in the V, Mn, and Fe chains would be a spin-spiral state. Furthermore, we evaluate the exchange-interaction parameters between the atoms and also spin-wave stiffness constants of all the atomic chains considered here from the calculated energy dispersion relations of the spin-spiral waves. The obtained exchange-interaction parameters allow us to understand why the spin-spiral state is stable in the V, Mn, and Fe chains but is not stable in the Cr, Co, and Ni chains. Finally, we also estimate the upper limits of the magnetic phase transition temperature for all the atomic chains.

This paper is organized as follows. After a brief description of the computational details in Sec. II, we present all the calculated energy dispersion relations of the spin-spiral waves of the 3*d* atomic chains in Sec. III. These results show that

a stable spin-spiral state exists in the V, Mn, and Fe chains. Reported in Sec. IV are the obtained exchange-interaction parameters, which enable us to understand the stability of the obtained magnetic ground state in each atomic chain considered. In Sec. V, we present the calculated spin-wave stiffness constant and also the estimated magnetic phase transition temperatures for the $3d$ atomic chains. Finally, the band structures of the spin-spiral state of the V and Mn chains are displayed in Sec. VI, and a summary of this work is given in Sec. VII.

II. THEORY AND COMPUTATIONAL METHOD

In the present first-principles calculations, we use the accurate frozen-core full-potential projector augmented-wave (PAW) method,[33] as implemented in the Vienna *Ab initio* Simulation Package (VASP).[34,35] The calculations are based on density functional theory, with the exchange and correlation effects being described by the generalized gradient approximation (GGA).[36] A very large plane-wave cutoff energy of 500 eV is used. The shallow core $3p$ electrons of the $3d$ transition metals are treated as valence electrons. We adopt the standard supercell approach to model an isolated atomic chain. The nearest wire and wire distance adopted here is 20 Å. We start with the theoretical equilibrium bond lengths for collinear magnetic states from our previous study of $3d$ transition metal (TM) nanowires.[24] However, in the fully unconstrained noncollinear magnetic calculations[37] for the spin spiral structures, we vary the bond length to study the bond length dependence of the stability of the spin spiral state. The Γ-centered Monkhorst-Pack scheme with a k mesh of $1 \times 1 \times n$ $(n = 100)$ in the full Brillouin zone (BZ), in conjunction with the Fermi-Dirac-smearing method with $\sigma = 0.02$ eV, is used for the BZ integration.

We consider the transverse spin-spiral states where all the spins rotate in a plane perpendicular to the spiral propagation vector $\mathbf{q}$. The total energies of the transverse spin spirals as a function of the magnitude of spin-spiral wave vector q are calculated self-consistently by using the generalized Bloch condition approach.[38,39] To study the exchange interactions, we apply the frozen-magnon approach and obtain the exchange-interaction parameters by a Fourier transformation of the energy spectra of the spin-spiral waves.

III. STABILITY OF SPIN-SPIRAL STATES

The calculated total energies $[E(q,\theta)]$ as a function of the spin-spiral propagation vector q of the $3d$ transition metal chains at several different bond lengths d are plotted in Fig. 1. Since we consider here the transverse spin-spiral waves only, the angle between the chain axis (i.e., z axis) and the magnetization direction $\theta = \pi/2$, and hence we simply write $E(q,\theta = \pi/2) = E(q)$. The spin-spiral structure at wave vector $q = 0$ corresponds to the collinear ferromagnetic (FM) state, while the state at $q = 0.5$ $(2\pi/d)$ corresponds to the antiferromagnetic (AF) state. Therefore, as shown in Fig. 1, at $q = 0$ the lowest total energy state of the Cr (Mn) chain occurs at 2.80 (2.60)Å, but it appears at 2.32 (2.29) Å at $q = 0.5$ $(2\pi/d)$, being in good agreement with our previous collinear magnetic calculations.[24] Interestingly, Fig. 1 shows that both

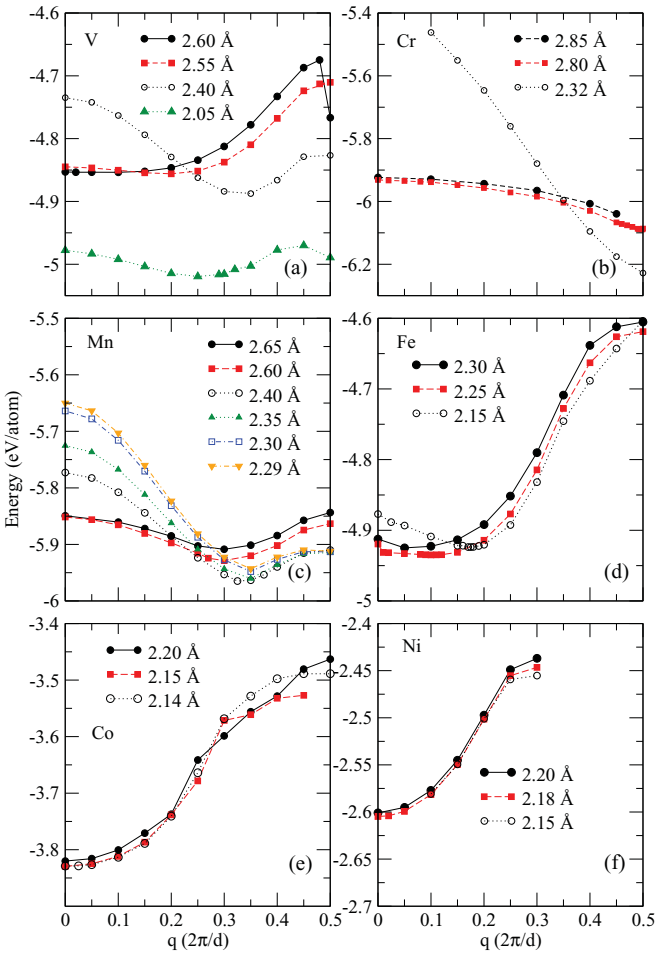

FIG. 1. (Color online) Total energy $E(q)$ vs spin-spiral wave vector q of the $3d$ transition metal chains at several different bond lengths d.

the FM and AF states in the V, Mn, and Fe chains become unstable against the formation of a spin-spiral structure. Furthermore, the lowest total energy of the spin-spiral state occurs at the bond length that is generally different from that of the collinear magnetic states. For example, the ground state of the Mn chain is the spin-spiral state with the equilibrium bond length of 2.40 Å instead of 2.60 (the FM state) and 2.29 Å (the AF state).[24]

Nonetheless, there is no stable spin-spiral state in the Cr, Co, and Ni chains. In the Cr chain, therefore, the AF state remains the stable state. In the Co and Ni chains, the FM state still has the lowest total energy (see Fig. 1). In fact, we could not even obtain a spin-spiral solution for the Ni chain at the wave vector q being larger than 0.3 $(2\pi/d)$. This is because, as shown in Fig. 1, an increase in the number of valence electrons leads to an increased stabilization of the FM state, while a decrease in the number of valence electrons tends to stabilize the AF state. This observation is further corroborated by the fact that in the Cr chain of bond length $d = 2.32$ Å, the total energy decreases steeply as the spin-spiral wave vector increases [Fig. 1(b)]. For comparison, we notice that in previous GGA calculations,[40] the FM state could not be stabilized in bulk Cr metal, while the magnetization energy of the AF state is rather small (~ 0.016 eV/at).

TABLE I. Calculated equilibrium bond length d, ground-state spin-spiral wave vector (q), and total energy [$E(q)$] [relative to that of the FM state ($q = 0$)] as well as spin magnetic moment (m_s) at $q = 0$ in the $3d$ transition metal chains. Note that the magnetic moment m_s and total energy $E(q)$ listed for the Cr chain are for the bond length $d = 2.80$ Å, since there is no stable FM state at $d = 2.32$ Å [see Fig. 1(b)].

	m_s (μ_B/at)	d (Å)	q ($2\pi/d$)	$E(q)$ (meV/at)
V	1.47	2.05	0.25	−166.4
Cr	4.18	2.32	0.50	−155.2
Mn	4.43	2.40	0.33	−113.3
Fe	3.30	2.25	0.10	−15.5
Co	2.18	2.15	0.00	
Ni	1.14	2.18	0.00	

The calculated equilibrium bond length (d), ground-state wave vector (q), and total energy [$E(q)$] as well as spin magnetic moment per unit cell (m_s) at $q = 0$ of all the $3d$ transition metal chains considered here are listed in Table I. We notice that the spin magnetic moment of the spin-spiral state of the V chain is significantly reduced, in comparison with the FM state (see Ref. 24), but is close to that of the AF state. Interestingly, Table I shows that the stable spin-spiral wavelength λ of the Fe chain is nearly exactly ten bond lengths (or lattice constant), while, in contrast, that for the V and Mn chains is much shorter, being four and three bond lengths, respectively. However, the spin-spiral wavelength λ can depend on the bond length, and this dependence is especially pronounced for the V chain, as demonstrated in Fig. 1(a). When the V chain is stretched to the bond length of 2.40 Å, the spiral propagation vector q becomes ∼0.35 ($2\pi/d$), but when it is further stretched to $d = 2.55$ Å, q is reduced to ∼0.20 ($2\pi/d$). A similar behavior of the spin-spiral wave vector can be found for the Fe chain, as shown Fig. 1(d).

The energy of a spin-wave excitation (i.e., the magnon dispersion relation) is given as the derivative of the total energy of the spin-spiral state with respect to the magnon number,[16,41]

$$\varepsilon(q) = \hbar\omega(q) = 2\mu_B \frac{\Delta E(\mathbf{q},\theta)}{\Delta M} = \frac{4\mu_B}{m_{s0}}[E(q) - E(0)], \tag{1}$$

where $\Delta E(q,\theta) = E(q,\theta) - E(0,\theta) = E(q) - E(0)$ is the energy of a spin spiral of wave vector $\mathbf{q}$ relative to the ferromagnetic state ($q = 0$), ΔM is the decrease of the magnetization per site projected onto the z axis, and m_{s0} is the spin magnetic moment per site at $q = 0$. The calculated magnon dispersion relations for the V, Cr, Mn, Fe, Co, and Ni chains at the minimal energy bond length are plotted in Fig. 2.

Ab initio calculations of the excitation energy of the spin-spiral wave along some high-symmetry lines in the Brillouin zone in bulk bcc Cr,[20] fcc Mn,[20] bcc Fe,[16–18,20] fcc Co,[16–18,20] and fcc Ni metals[16–18,20] have been reported before, and the stable spin-spiral structures were found in bcc Cr and fcc Mn. The stable spin-spiral wave with a wavelength of approximately seven lattice constants was also found in a free-standing bcc Fe(110) monolayer with lattice constant of 3.16 Å in two previous *ab initio* studies.[21,22] Here, we predict the existence of the stable spin-spiral structures in 1D free-standing transition metal (V, Mn ,and Fe) atomic chains.

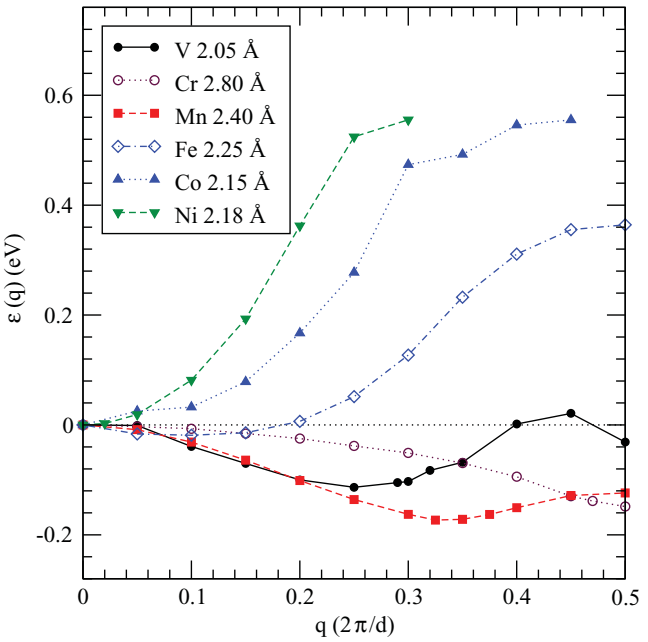

FIG. 2. (Color online) Calculated spin-wave energy spectra $\varepsilon(q)$ [i.e., magnon dispersion relations $\hbar\omega(q)$] of the $3d$ transition metal atomic chains at the ground-state bond length except the Cr chain where the bond length $d = 2.80$ Å is used.

IV. EXCHANGE INTERACTIONS

To a rather good approximation, we can map a metallic magnet onto an effective Heisenberg Hamiltonian with classical spins,[17,18]

$$H_{\text{eff}} = -\frac{1}{2}\sum_{i,j} J_{ij}\sigma_i \cdot \sigma_j, \tag{2}$$

where J_{ij} is an exchange interaction parameter between atomic site i and site j, and σ_i (σ_j) is the unit vector representing the direction of the local magnetic moment at site i (j). In the frozen magnon approach, the exchange-interaction parameters J_{ij} are related to the magnon excitation energy $\varepsilon(\mathbf{q})$ by a Fourier transformation,

$$J_{0j} = \frac{1}{N_{\mathbf{q}}}\sum_{\mathbf{q}} e^{-i\mathbf{q}\cdot\mathbf{R}} J(\mathbf{q}), \tag{3}$$

where $N_{\mathbf{q}}$ is the number of $\mathbf{q}$ points in the Brillouin zone included in the summation, and

$$\varepsilon(\mathbf{q}) = \frac{4\mu_B}{m_{s0}}[E(\mathbf{q}) - E(0)] = -\frac{2\mu_B}{m_{s0}}\sin(\theta)^2 J(\mathbf{q}) = -\frac{2\mu_B}{m_{s0}} J(\mathbf{q}). \tag{4}$$

Here, θ is fixed to $\pi/2$ for all the spin-spiral states and $J(\mathbf{q})$ is the Fourier transform of the exchange parameters. We therefore evaluate the exchange interactions in the $3d$ transition metal chains via Eqs. (3) and (4) by using the calculated magnon dispersion relations, as shown in Fig. 2.

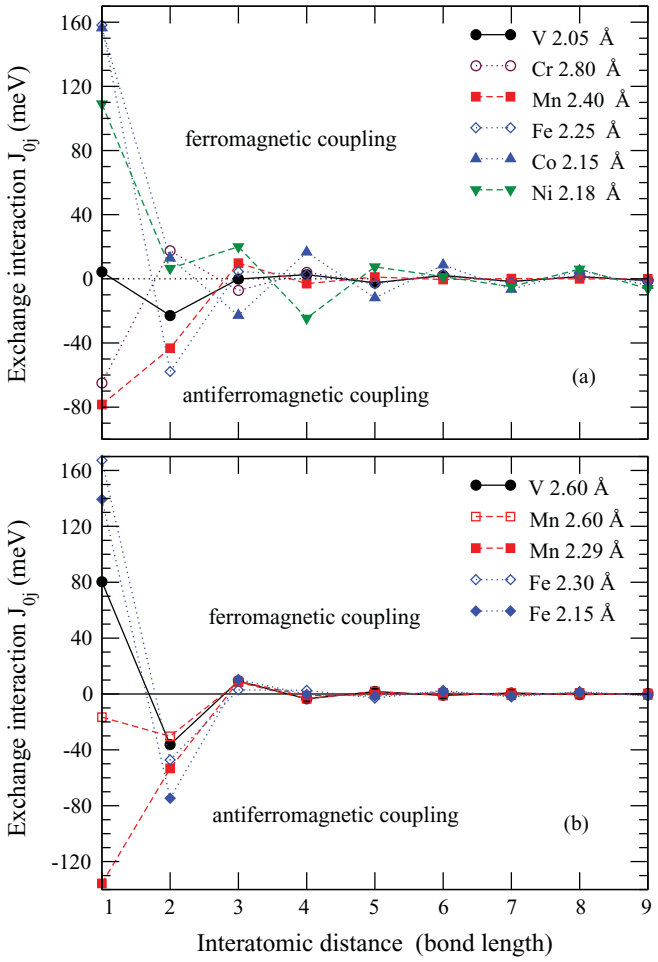

FIG. 3. (Color online) Calculated exchange-interaction parameters J_{0j} vs interatomic distance for the 3*d* transition metal chains with different bond lengths as labeled. In (a), the atomic chains are in their respective ground-state bond lengths except the Cr chain where the bond length $d = 2.80$ Å is used, and in (b), the atomic chains are in either stretched or compressed bond lengths.

The obtained exchange interaction parameters as a function of the interatomic distance are plotted in Fig. 3 and also listed in Table II. In the minimum energy bond lengths, as shown in Fig. 3(a), the magnetic coupling between the two first nearest neighbors in the V, Fe, Co, and Ni chains is ferromagnetic ($J_{01} > 0$), while it is antiferromagnetic ($J_{01} < 0$) in the Cr and Mn chains. In the Co and Ni chains, the magnetic coupling between the second nearest neighbors remain ferromagnetic ($J_{02} > 0$), and this explains why the ground state of these chains is ferromagnetic. In contrast, the magnetic coupling between the second nearest neighbors in the V, Mn, and Fe chains is antiferromagnetic ($J_{02} < 0$), i.e., the exchange interactions in these chains would be frustrated. As a result, noncollinear spin-spiral states in these chains may become energetically more favorable than either a collinear ferromagnetic or antiferromagnetic state. Let us take the Mn chain as an example, and consider the atomic spin at the origin. This spin tends to couple antiferromagnetically both with its two nearest neighbors and also with its two second nearest neighbors, because the first- and second-nearest-neighbor exchange parameters J_{01} and J_{02} are negative [see Fig. 3(a) and Table II]. However, this would make its two nearest-neighbor spins "frustrated" because they would have to couple ferromagnetically with one nearest neighbor on one side and antiferromagnetically with the other nearest neighbor on the opposite side. This frustrated magnetic coupling, therefore, would energetically favor a spin-spiral state. In fact, according to the mean-field theory for a 1D classical Heisenberg spin chain with negligibly small magnetic coupling between third nearest neighbors and beyond (see, e.g., Ref. 42), in the frustrated magnetic coupling situation ($J_{02} < 0$), the system would be ferromagnetic ($q = 0$) if $J_{01} > 4|J_{02}|$ and antiferromagnetic ($q = \pi/2$) if $J_{01} < -4|J_{02}|$. Table II shows clearly that the condition $J_{01} > 4|J_{02}|$ is fulfilled for the Co and Ni chains, giving rise to the ferromagnetic ground state. Interestingly, a stable spin-spiral structure with the spiral propagation vector q given by $\cos(qd) = -J_1/4J_2$ would occur if $J_{02} < 0$ and $4J_{02} < J_{01} < 4|J_{02}|$.[42] Using the exchange coupling parameters listed in Table II, we would obtain the spiral propagation vector $q = 0.24, 0.32$, and 0.13 $(2\pi/d)$, respectively, for the V, Mn, and Fe chains. These estimated q values agree very well with that obtained by the fully self-consistent total energy calculations (Table I).

TABLE II. Calculated exchange-interaction parameters (J_{0j}) (meV) between two jth near neighbors ($j = 1,2,3,4,5$) in the V, Cr, Mn, Fe, Co, and Ni atomic chains.

	J_{01}	J_{02}	J_{03}	J_{04}	J_{05}
V	4.2	−22.8	−0.2	2.6	−2.4
Cr	−65.0	17.6	−7.2	4.0	−2.6
Mn	−78.4	−43.2	9.8	−3.0	1.2
Fe	158.2	−57.8	4.4	2.6	−3.2
Co	156.4	13.0	−22.8	16.6	−11.8
Ni	109.0	6.6	20.0	−24.6	7.4

Figure 1 shows that the stability of the spin-spiral state in the V, Mn, and Fe chains depends pronouncedly on bond length d. Therefore, we also calculate the exchange-interaction parameters for these chains with several other bond lengths, and the results are plotted in Fig. 3(b). The equilibrium bond length for the FM V and Mn chains is 2.60 Å. The equilibrium bond lengths for the AF Mn and Fe chains are 2.29 and 2.15 Å, respectively. It is clear from Fig. 3 that the calculated exchange-interaction parameters can be sensitive to the bond length. For example, the magnitude of the nearest-neighbor exchange interaction J_{01} in the V atomic chain is dramatically increased from 2.1 to 40 meV as the bond length is increased from 2.05 to 2.60 Å. A similar behavior is found for the Fe chain (Fig. 3). Interestingly, in contrast, the magnitude of the nearest-neighbor exchange interaction J_{01} in the Mn chain is significantly reduced as the bond length is increased. Nevertheless, the exchange-interaction parameters for the second nearest neighbor and beyond are less affected by the bond length (see Fig. 3).

Ab initio evaluation of the exchange-interaction parameters in bulk ferromagnets Fe, Co, and Ni have been reported many times before. For example, the nearest-neighbor exchange interaction J_{01} in bcc Fe was determined to be 39.0 meV (Ref. 18) and 57.3 meV,[43] respectively. The nearest-neighbor exchange

interaction J_{01} in fcc Co was estimated to be 29.5 meV.[18] In bulk fcc Ni, the J_{01} was calculated to be 5.6 meV.[18] In the free-standing square Fe and Co monolayers with the Cu(001) lattice constant, the nearest-neighbor exchange interaction J_{01} is 92.5 and 77.6 meV,[11] respectively. These indicate that in 2D systems, in general, the exchange interactions are significantly enhanced as compared with their bulk counterparts, mainly because of reduced coordination numbers. Table II show that the nearest-neighbor exchange parameters J_{01} in the Fe, Co, and Ni chains are much larger than in their bulk counterparts. This may be attributed, at least partially, to the fact that the nearest bond length in the atomic chains is significantly shorter than in their bulk counterparts.[24] Our calculated J_{01} values in the Fe and Co chains are also significantly larger than the corresponding J_{01} values in the free-standing Fe and Co monolayers.[11] Interestingly, in the Fe atomic chains deposited on the Cu(117) surface, the effective exchange interaction parameter J_{eff} was determined to be around 136 meV,[44] being comparable with the corresponding J_{01} value of the free-standing Fe chain listed in Table II.

V. SPIN-WAVE STIFFNESS AND CRITICAL TEMPERATURE

The calculated energy dispersion relations of the spin-spiral waves $\varepsilon(q)$ for the $3d$ transition metal chains at the ground-state bond length are displayed in Fig. 2. In the range of small q, $\varepsilon(q) = Dq^2$, where the spin-wave stiffness constant D relates the spin-wave energy $\hbar\omega(q)$ to the wave vector q in the long-wavelength limit. The spin-wave stiffness constant D of an atomic chain can be estimated by fitting an even-order polynomial to the corresponding spin-wave spectrum shown in Fig. 2. The spin-wave stiffness constant D obtained in this way for the $3d$ metal chains is listed in Table III. A negative value of D means that the FM state is not stable against a spin-spiral wave excitation. Table III shows that the spin-wave stiffness constant D in the V, Cr, Mn, and Fe chains is negative. Only in the Co and Ni chains is D positive.

TABLE III. Calculated spin-wave stiffness constant D (meVÅ^2) and magnetic transition temperature T_C of the $3d$ metal chains. Also listed are the D's and T_C's for the 3D and 2D metal systems from previous *ab initio* calculations and experimental measurements for comparison.

	Stiffness D			T_C (K)		
	3D	2D	1D	3D	2D	1D
V			−424			94
Cr			−106	311[g]		414
Mn			−504			274
Fe	250,[a] 330[b]	164[c]	−78	1414,[a] 1043[d]	1265[c]	410
Co	663,[a] 510[b]	570[c], 427[e]	616	1645,[a] 1388[d]	1300[c]	606
Ni	756,[a] 555[f]		656	397,[a] 627[d]		458

[a]Theoretical calculations (Ref. 18).
[b]Neutron-scattering measurement extrapolated to 0 K (Ref. 45).
[c]Theoretical calculations (Ref. 11).
[d]Experimental measurements (Ref. 46).
[e]Brillouin light-scattering measurement (Ref. 47).
[f]Neutron-scattering measurement (Ref. 48).
[g]Neutron-scattering measurement (Ref. 49).

In principle, one can also calculate the spin-wave stiffness constant D via[16]

$$D = \frac{2\mu_B}{m_{s0}}\frac{d^2E(q)}{dq^2} = \frac{\mu_B}{3m_{s0}}\sum_j J_{0j}R_{0j}^2, \tag{5}$$

where J_{0j} are the exchange-interaction parameters and $R_{0j} = |\mathbf{R}_0 - \mathbf{R}_j|$ is the distance between site 0 and site j. In practice, Eq. (5) cannot be used directly to obtain reliable values for the spin-wave stiffness constant because the numerical uncertainties at the long distances are amplified by the factor R_{0j}^2.[18] Here we use this expression to understand the calculated D's listed in Table III. For example, the magnitude of the spin-stiffness constant D of the V chain is much larger than that of the Cr chain because the V chain has a much smaller spin magnetic moment (see Table I) and also a negative second-nearest-neighbor antiferromagnetic exchange parameter (see Table III). Furthermore, even though J_{01} is positive in the V and Fe chains, the D is negative, because the V and Fe chains have $J_{02} < 0$ and $J_{01} < 4|J_{02}|$.

For comparison, the spin-wave stiffness constants D's for the three-dimensional (3D) and two-dimensional (2D) Fe, Co, and Ni systems from previous *ab initio* calculations and experimental measurements are also listed in Table III. It is clear from Table III that the spin-wave stiffness constant tends to become smaller as the dimensionality of the system gets reduced. This may be expected [see Eq. (5)] because the number of near neighbors becomes smaller as the dimensionality of the system gets reduced. Among the three bulk $3d$ elemental ferromagnets, Fe has the smallest spin-wave stiffness, and, interestingly, the stiffness of Fe becomes negative when its dimensionality is decreased to 1 (Table III).

Within the mean-field (MF) approximation, the critical temperature (T_C) of the magnetic phase transition for the effective Heisenberg Hamiltonian can be estimated via the approximate expression[50,51]

$$k_B T_C^{\text{MF}} = \tfrac{1}{3}J(\mathbf{q}), \tag{6}$$

where $\mathbf{q}$ is the spin-spiral wave vector and $J(\mathbf{q})$ is the Fourier transform of the interatomic exchange parameters,

$$J(\mathbf{q}) = \sum_j J_{0j}e^{i\mathbf{q}\cdot\mathbf{R}_{0j}}. \tag{7}$$

In the ferromagnetic case ($\mathbf{q} = 0$),[50]

$$k_B T_C^{\text{MF}} = \frac{m_{s0}}{6\mu_B N_{\mathbf{q}}}\sum_{\mathbf{q}}\varepsilon(\mathbf{q}). \tag{8}$$

Using the calculated exchange-interaction parameters J_{0j} [Table III and Fig. 3(a)], and Eqs. (6) and (7), we estimate the transition temperatures T_C^{MF} for the $3d$ transition metal chains, as listed in Table III. Encouragingly, the ferromagnetic transition temperatures evaluated using Eq. (8) for the Co and Ni chains are 622 and 444 K, respectively, being in good agreement with that obtained using Eqs. (6) and (7) (Table III). Table III indicates that the critical temperature for the considered $3d$ atomic linear chains varies from several tens to a few hundreds of Kelvins. The critical temperatures for the $3d$ atomic chains are much smaller than the corresponding ones for the bulk metals and their monolayers (Table III). This is

due to the much reduced coordination numbers in these 1D systems, although the exchange interaction parameters in the atomic chains are generally larger than their counterparts in the bulks and monolayers.

The more accurate expression for the critical temperature within the random phase approximation (RPA) also exists,[11,50]

$$\frac{1}{k_B T_C^{\mathrm{RPA}}} = \frac{6\mu_B}{M}\frac{1}{N_q}\sum_q \frac{1}{\varepsilon(\mathbf{q})+\Delta}, \tag{9}$$

where Δ is the magnetic anisotropy energy. The RPA expression generally gives the critical temperatures for bulk ferromagnets Fe, Co, and Ni being in better agreement with experiments than the MF expression.[18] Furthermore, the critical temperatures with the MF approximation are usually significantly higher than that from the RPA calculations.[11,18] Using our calculated spin-wave dispersion relations (Fig. 2) and also the Δ values from Ref. 24, we obtain $T_C^{\mathrm{RPA}} = 230$ K for the Co chain and $T_C^{\mathrm{RPA}} = 229$ for the Ni chain. Therefore, the estimated critical temperatures listed in Table III should be considered only as the upper limits. Finally, we note that in the 1D isotropic Heisenberg model with finite-range exchange interactions, there is no spontaneous magnetization at any nonzero temperature because fluctuations become important.[52] Nonetheless, this discouraging conclusion has to be revised in the presence of a magnetic anisotropy and long-range interactions. Indeed, ferromagnetism in a 1D monatomic Co metal chain on a Pt substrate has been recently reported.[29] A detailed discussion on possible finite temperature spontaneous magnetization in 1D systems has been given in Ref. 53.

VI. ELECTRONIC BAND STRUCTURE

To study how the spin-spiral structure affects the electronic band structure[39] and also to help gain further insight into the spin-spiral instability at the microscopic level,[9,15] the electronic band structures of the V and Mn chains at several spin-spiral wave vectors q are displayed in Figs. 4 and 5, respectively. The ferromagnetic ($q = 0$) band structures are presented in Figs. 4 and 5(a). Because of the linear chain symmetry, the bands may be grouped into three sets, namely nondegenerate s- and d_{z^2}-dominant bands, doubly degenerate (d_{xz}, d_{yz}) bands, and ($d_{x^2-y^2}$,d_{xy}) dominant bands; see Figs. 4(a) and 5(a). The ($d_{x^2-y^2}$, d_{xy}) bands are narrow because the $d_{x^2-y^2}$ and d_{xy} orbitals are perpendicular to the chain, thus forming weak γ bonds. The d_{xz} and d_{yz} bands, on the other hand, are more dispersive due to the stronger overlap of the d_{xz} and d_{yz} orbitals along the chain, which gives rise to the π bonds. The s- and d_{z^2}-dominant bands are most dispersive since these orbitals form strong σ bonds along the chain.

Two main changes could appear in a ferromagnetic band structure when a spin-spiral wave is introduced, namely, the lifting of the accidental degeneracy at the cross-point of spin-up and spin-down bands and the "repulsion" of opposite-spin bands.[39] These changes can be clearly seen in Figs. 4(b) and 5(b). For example, in Fig. 4(b), the spin-up and spin-down d_{xz} and d_{yz} bands clearly move away from each other. Of course, these changes due to the noncollinear spin-spiral wave become more pronounced as q increases (Figs. 4 and 5). In the V chain, the repulsion of opposite-spin bands appears to lower

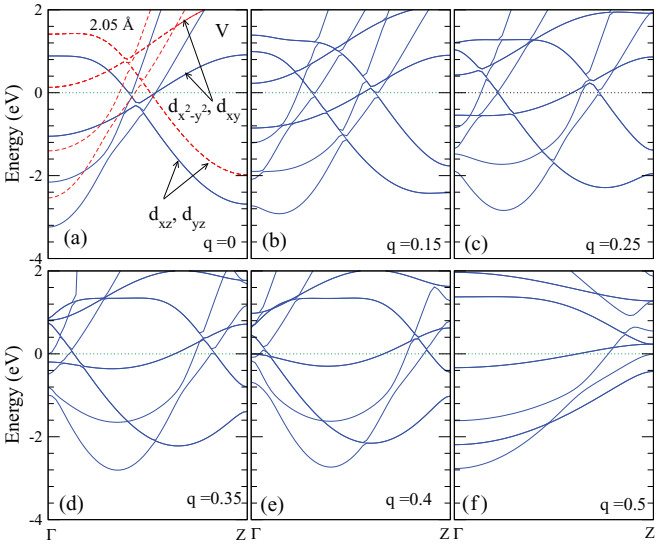

FIG. 4. (Color online) Band structures of the V chain in a different spiral propagation vector q along Γ to Z direction. In part (a), $q = 0$ ($2\pi/d$) indicates a spin-polarized ferromagnetic band structure, while in part (f), $q = 0.5$ ($2\pi/d$) indicates an AF band structure.

the spin-up d_{xz}-d_{yz} band considerably while at the same time raising the spin-down d_{xz} and d_{yz} bands significantly [see, e.g., Figs. 4(b) and 4(c)]. This could be the reason why the spin-spiral structure is energetically favored over the ferromagnetic state. In the Mn chain, on the other hand, as the wave vector q becomes nonzero, the fully occupied spin-up d_{xz}-d_{yz} band near the Γ point is pushed down substantially (see Fig. 5). This change could lead to a lowering of the total energy, thereby stabilizing the spin-spiral structure in the Mn chain. Figures 4 and 5 also show, in contrast, that as the spiral wave vector q becomes nonzero, the dispersive s- and d_{z^2}-dominant valence bands near the Γ point are pushed up in energy, and these shifts

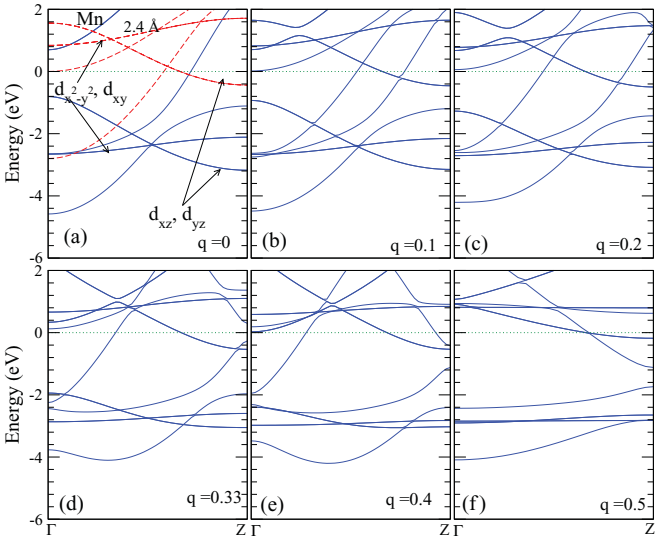

FIG. 5. (Color online) Band structures of Mn in a different spiral propagation vector q along Γ to Z direction. In part (a), $q = 0$ ($2\pi/d$) indicates a spin-polarized ferromagnetic band structure, while in part (f), $q = 0.5$ ($2\pi/d$) indicates an AF band structure.

are more or less proportional to the modulus of spin-spiral vector **q**. This upward movement of the s- and d_{z^2}-dominant bands might raise the total band energy. Therefore, the final equilibrium spiral wave vector q would be determined by a tradeoff of these two contrasting changes in the electronic band structure of the atomic chain.

VII. CONCLUSIONS

We have calculated the total energy of the transverse spin-spiral wave as a function of the wave vector for all 3d transition metal atomic chains within *ab initio* density functional theory with the generalized gradient approximation. As a result, we predict that at the equilibrium bond length, the V, Mn, and Fe chains have a stable spin-spiral structure. Furthermore, all the exchange interaction parameters of the 3d transition metal chains are evaluated by using the calculated energy dispersion relations of the spin-spiral waves. Interestingly, we find that the magnetic couplings in the V, Mn, and Cr chains are frustrated (i.e., the second near-neighbor exchange interaction is antiferromagnetic), and this leads to the formation of the stable spin-spiral structure in these chains. The spin-wave stiffness constant of these 3d chains is also evaluated and compared with its counterpart in bulk and monolayer systems. We have also estimated the upper limit of the possible magnetic phase transition temperature in these atomic chains within the mean-field approximation. The electronic band structure of the spin-spiral structures has also been calculated. We hope that our findings of the stable spin-spiral structure and frustrated magnetic interaction in the 3d transition metal chains will stimulate further theoretical and experimental research in this field. Indeed, after learning our *ab initio* results, Sandvik recently studied a spin-1/2 Heisenberg chain with both frustration and long-range interactions by exact diagonalization.[54] He found a first-order transition between a Néel state and a valence-bond solid with coexisting critical $k = \pi/2$ spin correlations.[54]

Note added in proof. Recently, we became aware of a recent theoretical work by Saubanere *et al.*[55] also studying the stability of spiral magnetic order in V nanowires.

ACKNOWLEDGMENTS

The authors thank A. W. Sandvik and Z. R. Xiao for stimulating discussions. The authors acknowledge support from the National Science Council and the NCTS of Taiwan. They also thank the National Center for High-performance Computing of Taiwan and the NTU Computer and Information Networking Center for providing CPU time.

*gyguo@phys.ntu.edu.tw

[1] Y. Kajiwara, K. Harii, S. Takahashi, J. Ohe, K. Uchida, M. Mizuguchi, H. Umezawa, H. Kawai, K. Ando, K. Takanashi, S. Maekawa, and E. Saitoh, Nature (London) **464**, 262 (2010).
[2] T. Lottermoser, T. Lonkai, U. Amann, D. Hohlwein, J. Ihringer, and M. Fiebig, Nature (London) **430**, 541 (2004).
[3] T. Kimura, T. Goto, H. Shintani, K. Ishizaka, T. Arima, and Y. Tokura, Nature (London) **426**, 55 (2003).
[4] S. T. Bramwell, S. R. Giblin, S. Calder, R. Aldus, D. Prabhakaran, and T. Fennell, Nature (London) **461**, 956 (2009).
[5] D. J. P. Morris, D. A. Tennant, S. A. Grigera, B. Klemke, C. Castelnovo, R. Moessner, C. Czternasty, M. Meissner, K. C. Rule, J.-U. Hoffmann, K. Kiefer, S. Gerischer, D. Slobinsky, and R. S. Perry, Science **326**, 411 (2009).
[6] S. Lounis, P. H. Dederichs, and S. Blügel, Phys. Rev. Lett. **101**, 107204 (2008).
[7] P. Ferriani, K. von Bergmann, E. Y. Vedmedenko, S. Heinze, M. Bode, M. Heide, G. Bihlmayer, S. Blügel, and R. Wiesendanger, Phys. Rev. Lett. **101**, 027201 (2008).
[8] H. Katsura, N. Nagaosa, and A. V. Balatsky, Phys. Rev. Lett. **95**, 057205 (2005).
[9] R. Lizárraga, L. Nordström, L. Bergqvist, A. Bergman, E. Sjöstedt, P. Mohn, and O. Eriksson, Phys. Rev. Lett. **93**, 107205 (2004).
[10] Y. Taguchi, Y. Oohara, H. Yoshizawa, N. Nagaosa, and Y. Tokura, Science **291**, 2573 (2001).
[11] M. Pajda, J. Kudrnovsky, I. Turek, V. Drchal, and P. Bruno, Phys. Rev. Lett. **85**, 5424 (2000).
[12] O. N. Mryasov, A. I. Liechtenstein, L. M. Sandratskii, and V. A. Gubanov, J. Phys. Condens. Matter **3**, 7683 (1991).
[13] Y. Tsunoda, J. Phys. Condens. Matter **1**, 10427 (1989).
[14] M. Uhl, L. M. Sandratskii, and J. Kübler, Phys. Rev. B **50**, 291 (1994).
[15] M. Körling and J. Ergon, Phys. Rev. B **54**, R8293 (1996).
[16] N. M. Rosengaard and B. Johansson, Phys. Rev. B **55**, 14975 (1997).
[17] S. V. Halilov, H. Eschrig, A. Y. Perlov, and P. M. Oppeneer, Phys. Rev. B **58**, 293 (1998).
[18] M. Pajda, J. Kudrnovsky, I. Turek, V. Drchal, and P. Bruno, Phys. Rev. B **64**, 174402 (2001).
[19] M. Marsman and J. Hafner, Phys. Rev. B **66**, 224409 (2002).
[20] S. Shallcross, A. E. Kissavos, V. Meded, and A. V. Ruban, Phys. Rev. B **72**, 104437 (2005).
[21] N. Mizuno, K. Nakamura, T. Akiyama, and T. Ito, J. Phys. Condens. Matter **19**, 365222 (2007).
[22] K. Nakamura, N. Mizuno, T. Akiyama, T. Ito, and A. J. Freeman, J. Appl. Phys. **99**, 08N501 (2006).
[23] D. C. Crew, R. L. Stamps, H. Y. Liu, Z. K. Wang, M. H. Kuok, S. C. Ng, K. Barmak, J. Kim, and L. H. Lewis, J. Magn. Mag. Mater. **290–291**, 530 (2005).
[24] J. C. Tung and G. Y. Guo, Phys. Rev. B **76**, 094413 (2007).
[25] J. C. Tung and G. Y. Guo, Phys. Rev. B **81**, 094422 (2010).
[26] H. Ohnishi, Y. Kondo, and K. Takayanagi, Nature (London) **395**, 780 (1998).
[27] A. I. Yanson, G. R. Bollinger, H. E. van der Brom, N. Agrait, and J. M. van Ruitenbeek, Nature (London) **395**, 783 (1998).
[28] V. Rodrigues, J. Bettini, P. C. Silva, and D. Ugarte, Phys. Rev. Lett. **91**, 096801 (2003).
[29] P. Gambardella, A. Dallmeyer, K. Maiti, M. C. Malagoli, W. Eberhardt, K. Kern, and C. Carbone, Nature (London) **416**, 301 (2002).
[30] S. B. Suh, B. H. Hong, P. Tarakeshwar, S. J. Youn, S. Jeong, and K. S. Kim, Phys. Rev. B **67**, 241402(R) (2003).
[31] J. C. Tung and G. Y. Guo, Comput. Phys. Commun. **182**, 84 (2011).
[32] J. C. Tung and G. Y. Guo (unpublished).

[33]P. E. Blöchl, Phys. Rev. B **50**, 17953 (1994); G. Kresse and D. Joubert, *ibid.* **59**, 1758 (1999).
[34]G. Kresse and J. Hafner, Phys. Rev. B **48**, 13115 (1993).
[35]G. Kresse and J. Furthmüller, Comp. Mater. Sci **6**, 15 (1996).
[36]Y. Wang and J. P. Perdew, Phys. Rev. B **44**, 13298 (1991); J. P. Perdew and Y. Wang, *ibid.* **45**, 13244 (1992).
[37]D. Hobbs, G. Kresse, and J. Hafner, Phys. Rev. B **62**, 11556 (2000).
[38]C. Herring, in *Magnetism*, edited by G. T. Rado and H. Suhl (Academic, New York, 1966).
[39]L. M. Sandratskii, J. Phys. Condens. Matter **3**, 8565 (1993); **3**, 8587 (1993).
[40]G. Y. Guo and H. H. Wang, Phys. Rev. B **62**, 5136 (2000).
[41]Q. Niu, X. Wang, L. Kleinman, W.-M. Liu, D. M. C. Nicholson, and G. M. Stocks, Phys. Rev. Lett. **83**, 207 (1999).
[42]J. D. Patterson and B. C. Cailey, *Solid-State Physics*, Introduction to the Theory (Springer, New York, 2007).
[43]J.-T. Wang, L. Zhou, D.-S. Wang, and Y. Kawazoe, Phys. Rev. B **62**, 3354 (2000).
[44]D. Spisák and J. Hafner, Phys. Rev. B **65**, 235405 (2002).
[45]P. Pauthenet, J. Appl. Phys. **53**, 8187 (1982).
[46]N. W. Ashcroft and N. D. Mermin, *Solid State Physics* (Holt, Rinehart and Winston, New York, 1976).
[47]Y. Akira, J. Magn. Soc. Jpn. **28**, 1023 (2004).
[48]H. A. Mook, J. W. Lynn, and M. R. Nicklow, Phys. Rev. Lett. **30**, 556 (1973).
[49]E. Fawcett, Rev. Mod. Phys. **66**, 25 (1994).
[50]C. S. Wang, R. E. Prange, and V. Korenman, Phys. Rev. B **25**, 5766 (1982).
[51]J. Jensen and A. R. Mackintosh, *Rare Earth Magnetism* (Clarendon, Oxford, 1991).
[52]N. D. Mermin and H. Wagner, Phys. Rev. Lett. **17**, 1133 (1966).
[53]S. Curilef, L. A. del Pino, and P. Orellana, Phys. Rev. B **72**, 224410 (2005).
[54]A. W. Sandvik, Phys. Rev. Lett. **104**, 137204 (2010).
[55]M. Saubanere, M. Tanveer, P. Ruiz-Diaz, and G. M. Pastor, Phys. Status Solidi B **247**, 2610 (2010).